Journal of Computational Electronics X:YYY-ZZZ,200?
©Kluwer Academic Publishers *Manufactured in The Netherlands*

Efficient Simulation of the Full Coulomb Interaction in Three Dimensions

CLEMENS HEITZINGER, CHRISTIAN RINGHOFER
Department of Mathematics, Arizona State University, Tempe, AZ 85287, USA
Clemens.Heitzinger@asu.edu

SHAIKH AHMED, DRAGICA VASILESKA
Department of Electrical Engineering, Arizona State University, Tempe, AZ 85287, USA
Dragica.Vasileska@asu.edu

Abstract. The full Coulomb interactions, i.e., electron-electron and electron-impurity interactions, play an important role in the operation of ultra-small MOSFETs. Previous simulation approaches (particle-mesh and particle-particle particle-mesh methods) were found to be very time consuming because of the imposed boundary conditions. In this work it is proposed to use a fast multi-pole method instead whose applicability is verified in bulk mobility and device simulations. It is found that this approach yields physically correct results and accounts for all Coulomb interactions in the device within significantly decreased simulation times.

Keywords: Monte Carlo simulation, full Coulomb interaction, electron-electron interactions, discrete impurity effects, fast multi-pole method, nanoscale semiconductor devices, ultra-small MOSFETs.

1. Introduction

The continued scaling of MOSFETs into the nanoscale regime requires refined models for carrier transport. One reason is unintentional doping in the active channel region which gives rise to threshold voltage and on-state current fluctuations. Electron-electron interactions affect the threshold voltage, the carrier dynamics, and the device characteristics [1, 2].

Therefore every transport simulator which is supposed to accurately simulate nano-devices must model the full Coulomb interaction properly. In a typical Poisson-EMC (Ensemble Monte Carlo) transport simulation sequence the long range part of the Coulomb interaction due to both the electron-electron and electron-impurity interactions is handled by solving the Poisson equation repeatedly. The short range part of the interactions is included in the k-space part of the EMC transport sequence. This approach is impractical for two reasons.

Firstly the separation of the Coulomb interaction in a short and a long range component is inaccurate and the long range part may depend on the mesh size. Non-uniformity in the source distributions can cause degradation of performance and errors may originate from the numerical differentiation used to calculate the field from the mesh potential depending on the scheme to couple a particle to the mesh. Secondly the k-space treatment of the short range part is inaccurate, since it is necessary to know the distribution function to accurately describe the screening. The evaluation of the distribution function is, in turn, rather CPU intensive and noisy because of the poor statistics usually found in realistic device structures.

Hence a real space treatment of the short range interactions has been proposed. Variants thereof are the P^{3}M (particle-particle particle-mesh) method [3, 4], adapted to the boundary conditions necessary for semiconductor devices, and the corrected Coulomb approach [1, 5]. Although real space treatments eliminate the problem of double counting the force, a drawback is that the Poisson equation must be solved repeatedly to properly describe the self-consistent fields which consumes over 80% of the total time spent in

3D simulations.

Furthermore, when P^3M methods are applied to simulations of semiconductor devices, their drawbacks are twofold. Firstly FFT cannot be used to solve the Poisson equation since the boundary conditions are non-periodic. Secondly the inverse of the Laplace operator must be calculated for each particle in order to prevent counting nearby particles twice which is, of course, very time consuming. In order to alleviate this problem the inverse can be precomputed (which takes several hours) and stored (which requires lots of memory), but this must be repeated for every new device structure.

2. Simulation Method

To overcome all of the above mentioned issues and to further speed up simulations, we propose to use a 3D FMM (fast multi-pole method) [6, 7, 8, 9] instead. The FMM allows to find the field and potential in a system of n particles connected by a central force within $O(n)$ time to a certain prescribed accuracy. For our applications this means that all Coulomb field effects can be included.

The FMM is based on the idea of condensing the information of the potential generated by point sources in truncated series expansions. After calculating suitable expansions, the long range part of the potential is obtained by evaluating the truncated series at the point in question and the short range part is calculated by direct summation. Its computational effort is only $O(n)$, where n is the number of particles, instead of being proportional to $\binom{n}{2}$ for direct summation.

The field due to the applied boundary biases is obtained at the beginning of the simulation by solving the Poisson equation. Hence the total field acting on each electron is the sum of this constant field and the contribution from the electron-electron and electron-impurity interactions handled by the FMM calculations. Care must be taken when choosing the time step. If it is too large, electrons may approach one another and impurities too closely which yields non-physically high forces and hence too high velocities and energies. To avoid this artificial numerical heating we use a cut-off range of 1 nm for the Coulomb force.

In electrodynamics it is well-known that in non-homogeneous media the Coulomb force between two particles must be corrected, which is usually achieved by the introduction of image charges [10, 11]. It is trivial to include the ghost charges in the FMM algorithm. They are added to the list of charges being considered. The algorithm proceeds normally, but in the end the image charges are neglected when the field and potential are evaluated.

3. Simulation Results and Discussion

To check the physical validity and speed of the FMM approach, we first simulated an n^+–n–n^+ resistor [12] using our 3D EMC device simulator [5, 13]. The theoretically calculated results for the low-field electron mobility using the P^3M, the corrected Coulomb, the FMM, the PM (particle-mesh), and the Brooks–Herring k-space approach (bulk MC) were compared with available experimental data [14]. In summary it was found that the low-field mobility calculated with the FMM approach agrees very well with the experimental values for both low and high doping concentrations. The k-space Brooks–Herring approach significantly overestimates the low-field electron mobility for high substrate doping densities and the PM approach yields completely wrong results. Furthermore the simulation times were halved when using the FMM compared to the P^3M approach. Further results for 2D devices are reported in [15].

We also checked the speed of the FMM approach on two different examples of SOI device structures. The first device has a silicon film thickness of 25 nm, a channel width of 30 nm, an oxide thickness of 4 nm, a channel length of 50 nm, and channel doping equal to $10^{18}\,\mathrm{cm}^{-3}$. Its structure is shown in Figure 1. To simulate this device structure a mesh size of 5 nm that resulted in $22 \cdot 20 \cdot 15$ mesh nodes was used. Based on the doping of the source and drain regions the device contained approximately 7500 electrons.

There are several noteworthy conclusions that can be drawn from the results shown in Figure 2. Firstly the use of the mesh force alone, i.e., the PM method, leads to higher current levels, which suggests that one can overestimate the performance of the device if one does not take the short range parts of the Coulomb interaction into account. Secondly the corrected Coulomb, the P^3M, and the FMM approaches yield approximately the same values for the current density. Thirdly the CPU time needed to calculate one bias point by using the P^3M approach is about twice the time required by the FMM. Hence the FMM–EMC device simulation scheme leads to physically accurate results, but requires only half the simulation time.

The next question is what happens when even smaller device structures are considered. When using a self-consistent EMC device simulator for small

devices, one must use very small mesh sizes in order to resolve the device geometry properly. This implies a large number of node points ($100 \cdot 22 \cdot 30$ in the following example). On the other hand the systems are so small that only very few electrons participate in the transport. Hence it is quite natural to expect that under such circumstances the FMM–EMC device simulator will perform even better.

To check this point we simulated a narrow-width SOI device with a silicon film thickness of 7 nm, a channel width of 10 nm, an oxide thickness of 34 nm, a channel length of 50 nm, and channel doping equal to $10^{16}\,\mathrm{cm}^{-3}$. The doping of the source-drain regions is taken to be equal to $5 \cdot 10^{19}\,\mathrm{cm}^{-3}$. The results of these simulations are presented in Figures 4 and 5. It is found that the use of a smaller mesh size captures a great percentage of the short range Coulomb interactions, so the PM data are much closer to the corrected Coulomb, the $\mathrm{P}^3\mathrm{M}$, and the FMM data. Furthermore the CPU time needed to calculate one bias point with the FMM–EMC was five times smaller than the time needed by the $\mathrm{P}^3\mathrm{M}$ approach, i.e., the simulation time was reduced from approximately five hours to less than one hour on current hardware.

4. Conclusion

In summary the use of FMM for semiconductor transport simulations was validated. Simulation times are decreased significantly, short and long range electron-electron and electron-impurity interactions are handled in a rigorous manner, and effects due to electron-electron and electron-impurity interactions are observed as expected. Since the FMM algorithm operates independently of the rest of the EMC simulation, it can be easily included into existing EMC device simulation codes.

This approach is very efficient concerning simulation time avoiding the drawbacks inherent in the $\mathrm{P}^3\mathrm{M}$ approach. In our simulations of different 3D device geometries we observed speed-ups in the range of factors from 2 to 20, where factors of 10 can usually be expected.

Additionally this approach leads to mesh-less 3D EMC particle-based device simulators. Since the simulator operates without any mesh (except for the initial solution of the Poisson equation that stays constant during the whole simulation), the question of how to choose the mesh size does not arise. In practice this means greater confidence in simulation results without the need to check the dependence of simulation results on mesh size.

Finally this approach will work better and better for future technologies, i.e., smaller devices. Smaller devices require finer meshes and therefore the FMM–EMC simulator will have an even greater speed advantage.

5. Acknowledgment

The first author acknowledges support by the Austrian Science Fund (Fonds zur Förderung der wissenschaftlichen Forschung, FWF) via an Erwin Schrödinger Fellowship. The authors also acknowledge support from NSF under contract No. ECS 021-8008.

References

Elements of this work have been summarized in an extended abstract published by IEEE.

1. W.J. Gross, D. Vasileska, and D.K. Ferry. A novel approach for introducing the electron-electron and electron-impurity interactions in particle-based simulations. *IEEE Electron Device Lett.*, 20(9):463–465, September 1999.
2. W.J. Gross, D. Vasileska, and D.K. Ferry. Ultrasmall MOSFETs: The importance of the full coulomb interaction on device characteristics. *IEEE Trans. Electron Devices*, 47(10):1831–1837, October 2000.
3. A.S. Sangani and G. Mo. An $O(N)$ algorithm for Stokes and Laplace interactions of particles. *Phys. Fluids*, 8(8):1990–2010, August 1996.
4. C.J. Wordelman and U. Ravaioli. Integration of a particle-particle-particle-mesh algorithm with the ensemble monte carlo method for the simulation of ultra-small semiconductor devices. *IEEE Trans. Electron Devices*, 47(2):410–416, February 2000.
5. W.J. Gross, D. Vasileska, and D.K. Ferry. Three-dimensional simulations of ultra-small MOSFETs with real-space treatment of the electron-electron and electron-ion interactions. *VLSI Design*, 10:437–452, 2000.
6. L. Greengard and V. Rokhlin. A fast algorithm for particle simulations. *J. Comput. Phys.*, 135(2):280–292, 1997.
7. R. Beatson and L. Greengard. A short course on fast multipole methods. In *Wavelets, Multilevel Methods and Elliptic PDEs (Leicester, 1996)*, Numer. Math. Sci. Comput., pages 1–37. Oxford Univ. Press, New York, 1997.
8. H. Cheng, L. Greengard, and V. Rokhlin. A fast adaptive multipole algorithm in three dimensions. *J. Comput. Phys.*, 155(2):468–498, 1999.
9. MadMax Optics, Hamden, CT, USA. *FMMPART3D user's guide*, version 1.0 edition.
10. J.D. Jackson. *Classical Electrodynamics.* Wiley, 3rd edition, 1998.
11. J.S. Schwinger et al. *Classical Electrodynamics.* Perseus, 1998.
12. Clemens Heitzinger, Christian Ringhofer, Shaikh Ahmed, and Dragica Vasileska. Accurate three-dimensional simulation of electron mobility including electron-electron and

electron-dopant interactions. In *Proc. 206th Meeting of the Electrochemical Society (ECS)*, Honolulu, HI, USA, October 2004. The Electrochemical Society. *(In print)*.

13. D. Vasileska and S.M. Goodnick. Computational electronics. *Materials Science and Engineering Reports*, R38(5):181–236, 2002.
14. C. Canali, G. Ottaviani, and A. Alberigi-Quaranta. Drift velocity of electrons and holes and associated anisotropic effects in silicon. *J. Phys. Chem. Solids*, 32:1707, 1971.
15. Clemens Heitzinger, Christian Ringhofer, Shaikh Ahmed, and Dragica Vasileska. On the efficient simulation of electron-electron interactions in nanoscale MOSFETs. *Nanotechnology*, April 2005. *(In print)*.

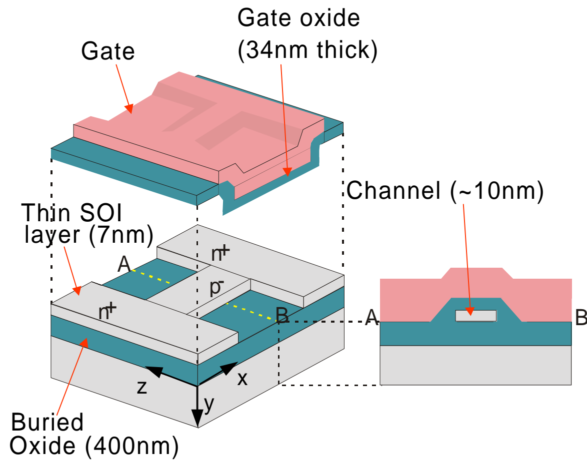

Figure 1: The device structure of the SOI MOSFET.

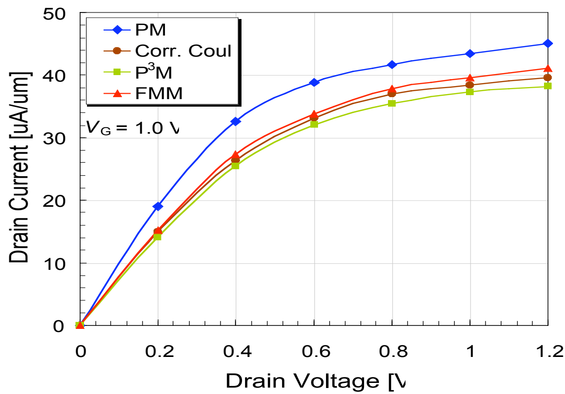

Figure 2: The I_d–V_d curve of the first SOI device for an applied gate bias of $V_g = 1.0\,\mathrm{V}$ as obtained by the PM, the corrected Coulomb, the P^{3}M, and the FMM methods.

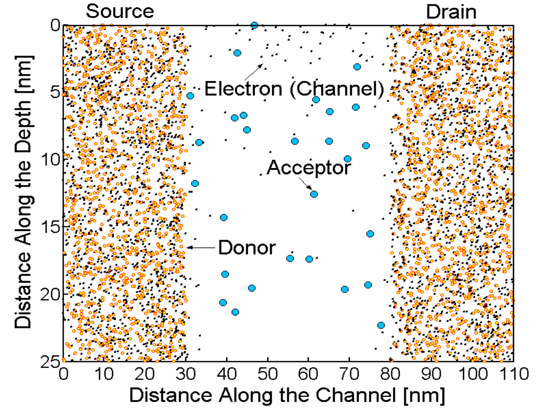

Figure 3: The position of dopants and electrons during an FMM–EMC simulation of the first device corresponding to Figure 2.

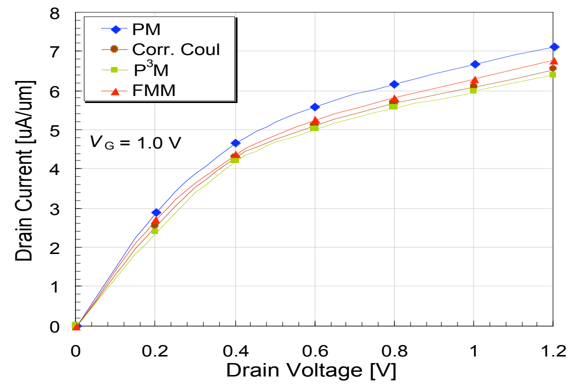

Figure 4: The I_d–V_d curve of the second SOI device for an applied gate bias of $V_g = 1.0\,\mathrm{V}$ as obtained by the PM, the corrected Coulomb, the P^{3}M, and the FMM methods.

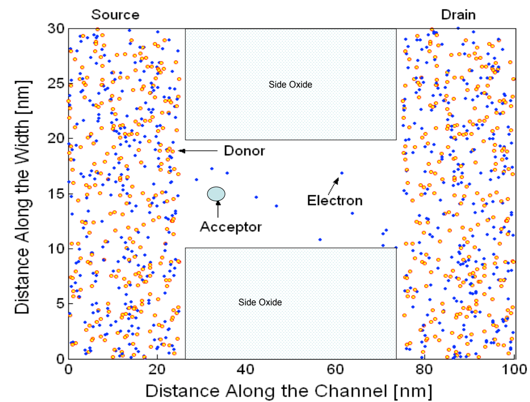

Figure 5: The position of dopants and electrons during an FMM–EMC simulation of the second device corresponding to Figure 4.